DTM-PADE APPROACH TO MHD SLIP FLOW AND HEAT TRANSFER OVER A RADIALLY STRETCHING SHEET WITH THERMAL RADIATION

S.R. SAYYED†, B.B. SINGH†, O.D. MAKINDE‡ and NASREEN BANO†

† *Department of Mathematics, Dr. Babasaheb Ambedkar Technological University, Lonere-402103, Dist. Raigad(M.S.), India. Email: srsayyed786@gmail.com, bbsingh@dbatu.ac.in, snasreenbano@yahoo.in*

‡ *Faculty of Military Science, Stellenbosch University , South Africa. Email: makinded@gmail.com*

***Abstract*— The present paper deals with the boundary layer flow and heat transfer of an electrically conducting magnetohydrodynamic viscous fluid over a radially stretching power-law sheet with suction/injection within a porous medium by considering the effects of momentum and thermal slips and thermal radiation. The governing non-linear partial boundary layer differential equations are reduced to a system of coupled non-linear ordinary differential equations (ODEs) with the aid of appropriate similarity transformations. These transformed ODEs are then solved by employing a semi-analytic technique known as differential transformation method (DTM) in combination with Pade approximation. The numerical values of skin friction and local Nusselt number are tabulated and validated by comparing them with the corresponding values available in the literature. Our results have been found in precise agreement with the results published earlier. The effects of different governing parameters on velocity and temperature distributions are analyzed graphically. It has been found that with an increase in the velocity slip parameter the fluid velocity decreases, whereas the temperature of the fluid increases. Also, the fluid temperature gets enhanced with an increase in the radiation parameter, but it decreases with an increase in thermal slip.**

***Keywords*—DTM method, MHD flow, Heat transfer, Velocity slip, Thermal slip, Thermal Radiation.**

I. INTRODUCTION

The study of boundary layer flow and heat transfer of a viscous fluid over a continuous stretching sheet, in recent years, has been a topic of attraction among various researchers due to its significant applications in manufacturing industries such as extrusion of plastic and rubber, polymer and metal processing, wire drawing, annealing and thinning of copper wire, glass-fibre and paper production, etc.

In this area, Sakiadis (1961) did a pioneering work in order to study the boundary layer flows over continuous solid surfaces. Crane (1970) was amongst the first to give a closed form solution of the laminar flow over a linearly stretching sheet. This study was then extended by Chen and Char (1999) by including the heat and mass transfer effects with suction and injection. The investigation of the flow and heat transfer problems over a linearly stretching sheet is carried out by a number of researchers like Andersson (1992), Cortell (1994), Ariel (2001), Liao (2003), Cortell (2005), Cortell (2006), Hayat *et al*. (2006). Gupta and Gupta (1977) reported that realistically, the sheet stretching needs not be linear. As a matter of this fact only, many a researchers like Magyari and Keller (1999), Vajravelu and Cannon (2006), etc. have dealt with the problems wherein the sheets are non-linear, especially exponential, in configuration. Furthermore, as the sheet can be stretched in a number of ways, the flow past a stretching sheet may not be necessarily two-dimensional. For example, a sheet can also be stretched radially. In this reference, Sajid *et al*. (2008) investigated the axisymmetric unsteady flow and heat transfer over a radially stretching sheet. In a similar manner, many other researchers like Shahzad *et al*. (2012), Shateyi and Makinde (2013), Hayat *et al*. (2015), Khan *et al.* (2015a), Makinde *et al.* (2016), Ahmed *et al.* (2016), Khan *et al.* (2015b), etc. have paid their attention towards the study of flow and heat transfer problems over radially stretching sheets.

All the above mentioned studies have been carried out by taking into account the no-slip boundary condition. The no-slip boundary condition is one of the core principles of the Navier-Stokes' theory which is based on the assumption of adherence of a fluid to a solid body. In several situations, however, the no-slip boundary condition cannot be applied and should be replaced by partial slip boundary condition. The particulate fluids such as suspensions, emulsions, polymer solutions and foams, etc. exhibit the partial slip on the stretching boundary. The velocity slip, i.e. the inadequacy of the no-slip on a solid boundary, is a phenomenon that has been seen under certain circumstances mentioned by Yoshimura and Prud'homme (1988).

The study of fluids exhibiting the boundary slip condition has some significant technological applications such as in the polishing of artificial heart valves and internal cavities. In some coated surfaces like Teflon, which resist adhesion, the Navier's partial slip condition is considered where the slip velocity is proportional to the local shear stress. However, experiments suggest that the slip velocity also depends on the normal stress. A number of problems have been modeled for describing the slip occurring at the solid boundary e.g. Andersson (2002), Ariel *et al.* (2006), Abbas *et al.* (2009), etc. A new dimension is added to the above mentioned studies by taking into account the partial slip condition at the stretching boundary. Representative studies dealing with such effects can also be found in the works of Turkyilmazoglu (2015a, 2015b, 2019), Sahoo (2010) and Mukhopadhyay and Gorla (2012).

Moreover, the radiation heat transfer studies play a vital role from the application view point in the various fields of physics and engineering like in space technology and high temperature processes. Also, thermal radiation effects are applicable in polymer industries, where the quality of the final product depends on the heat controlling factors. High temperature plasmas, cooling of nuclear reactors, liquid metal fluids, magnetohydrodynamic accelerators, power generation systems, etc. are some other applications of the radiative heat transfer from a vertical wall. Due to these reasons only, the essentials of radiative heat transfer can be found in the works of Sparrow and Cess (1970) and Vafai *et al*. (2000). Many other pertinent radiative heat transfer studies for different configurations have been reported by researchers like Hossain and Takhar (1996), Raptis (1998), Makinde and Moitsheki (2008), Mukhopadhyay (2009), Sibanda and Makinde (2010), Makinde and Aziz (2010), Makanda *et al.* (2013), Das *et al.* (2017), Gangadhar *et al.* (2018).

The differential transform method (DTM), developed by Zhou (1986), who tackled the problem of linear and non-linear differential equations arising in electric circuit analysis, is an iterative procedure which gives analytic solutions of ordinary and partial differential equations in a way of polynomial. The use of DTM is advantageous as it is less time consuming and it reduces the rigorous calculations to be performed for obtaining the Taylor series. This method can also be applied to non-linear differential equations without the aid of linearisation, discretization and perturbation. As a consequence of this, this scheme was extended by Chen and Ho (1999) for solving partial differential equations. Therefore, Ayaz (2004) used it to investigate the system of differential equations. Arikoglu and Ozkol (2006) applied it to difference equations. Darania and Ebadian (2007) applied it to integro- differential equations. Rashidi (2009) applied this method for solving the MHD boundary layer equations. All these successful applications of the DTM verify its validity, effectiveness and flexibility. Though the results obtained by DTM in case of the differential equations on unbounded domains are valid in small region, but in a wider range they are invalid. It happens due to the divergent nature of the closed series solutions investigated by DTM when the independent variable of the problem tends to infinity. Boyd (1997) and other researchers have also proved that the power series in unbounded domains is not useful for handling boundary value problems. But, Su and Zheng (2011) used the DTM in combination with the Pade technique successfully to overcome such a difficulty and could find the approximate solutions for a wider range.

It is found from the existing literature that no attention has been paid till date towards the investigation of the effects of partial slip and thermal radiation on flow and heat transfer problems over radially stretching power-law sheets in porous medium. Hence, the objective of the present study is to analyze the MHD flow and heat transfer of a viscous fluid over a porous radially stretching sheet by taking the partial slips and radiative fluid properties into consideration. To validate the accuracy of the results obtained by the DTM-Pade method, our numerical values of the skin friction coefficient and the Nusselt number have been compared with the corresponding values of Khan et al. (2015b) who tackled the same problem in the absence of thermal radiation and partial slips by using the Homotopy analysis method (HAM) for analytical solutions, and shooting technique for numerical solutions. The results have been found in precise agreement. The effects of various governing parameters on the velocity and temperature fields are sketched graphically and then discussed.

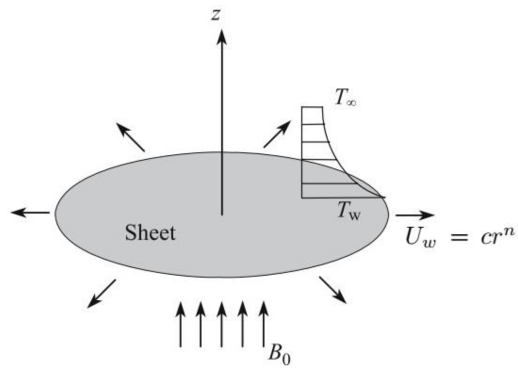

Figure 1: Schematic diagram of the flow

II. PROBLEM FORMULATION

Let us consider the MHD flow and heat transfer of a viscous, incompressible and electrically conducting fluid over a porous radially stretching power-law sheet coinciding the plane $z = 0$. In the flow process, the magnetic Reynolds number is assumed to be very small so as to ignore the effects of induced magnetic field. The sheet is stretched along the radial direction with a velocity $U_w = c\, r^n$, where c is a constant and r is the radial coordinate, and the flow is confined in the region $z > 0$. We also assume that the surface of the sheet is at constant temperature T_w with the uniform ambient fluid temperature T_∞, where $T_w > T_\infty$. It is further assumed that the uniform magnetic field $B = [0, 0, B_0]$ acts normal to the sheet i.e. along z- axis. The fluid adheres to the sheet partially and thus the motion of the fluid exhibits slip condition (see Fig. 1).

Under these assumptions, the governing boundary layer equations for the flow and heat transfer of a viscous fluid in terms of cylindrical coordinates take the form (cf. Khan *et al.*, 2015a)

$$\frac{\partial u}{\partial r} + \frac{u}{r} + \frac{\partial w}{\partial z} = 0, \tag{1}$$

$$u\frac{\partial u}{\partial r} + w\frac{\partial u}{\partial z} = \nu\frac{\partial^2 u}{\partial z^2} - \sigma\frac{B_0^2}{\rho}u - \frac{\nu\phi}{k}u, \tag{2}$$

$$u\frac{\partial T}{\partial r} + w\frac{\partial T}{\partial z} = \alpha\frac{\partial^2 T}{\partial z^2} - \frac{1}{\rho c_p}\frac{\partial q_r}{\partial z}, \tag{3}$$

where u and w are the velocity components along the radial and axial directions, respectively; B_0 is a constant applied magnetic field in z-direction; ρ is fluid density;

σ is the electrical conductivity; T is temperature of the fluid; $\alpha = k_1/(\rho c_p)$ is the thermal diffusivity; k_1 is thermal conductivity; ν is the kinematic viscosity; k is permeability of the porous medium; ϕ is porosity; c_p is the specific heat at constant pressure, and q_r is the radiative heat flux.

Using the Rosseland approximation for radiation given by Brewster (1992), one can write

$$q_r = -4\frac{\gamma^*}{3\,k^*}\left(\frac{\partial T^4}{\partial z}\right),$$

where γ^* is the Stefan-Boltzmann constant and $k^*$is absorption coefficient.

Assuming that the temperature difference within the flow is such that T^4 may be expanded in a Taylor series about T_∞, the free stream temperature after neglecting higher order terms can be linearized to obtain

$$T^4 \approx 4\,T_\infty^3\,T - 3T_\infty^4$$

So, the Eq.(3) becomes

$$u\frac{\partial T}{\partial r} + w\frac{\partial T}{\partial z} = \alpha\frac{\partial^2 T}{\partial z^2} + \frac{16\,\gamma^*\,T_\infty^3}{3\rho c_p k^*}\left(\frac{\partial^2 T}{\partial z^2}\right). \qquad (4)$$

The appropriate boundary conditions on the flow are

$$\left.\begin{aligned} u &= cr^n + l_1\frac{\partial u}{\partial z},\ w = -V_w, \\ T &= T_w + d_1\frac{\partial T}{\partial z} \quad at\ z = 0, \\ u &\to 0,\ T = T_\infty \quad as\ z \to \infty, \end{aligned}\right\} \qquad (5)$$

where $V_w > 0$ is the suction velocity, $V_w < 0$ gives the injection velocity; l_1 is the velocity slip factor; d_1 is the thermal slip factor, and n is a power-law constant called stretching parameter.

We now introduce the following similarity transformations

$$\left.\begin{aligned} \eta &= \frac{z}{r}\,(Re)^{\frac{1}{2}}\,, \\ \psi(r,z) &= -r^2\,U_w\,Re^{-\frac{1}{2}}\,f(\eta)\,, \\ \theta(\eta) &= \frac{T-T_\infty}{T_w-T_\infty}, \end{aligned}\right\} \qquad (6)$$

where η is the dimensionless similarity variable; $Re = rU_w/\nu$ is the local Reynolds number depending on r, and $\psi(r,z)$ is the Stokes stream function defined as

$$u = -\frac{1}{r}\frac{\partial\psi}{\partial z}, \qquad w = \frac{1}{r}\frac{\partial\psi}{\partial r},$$

which gives

$$\left.\begin{aligned} u &= U_w f'(\eta), \\ w &= -U_w\,Re^{-\frac{1}{2}}\left(\frac{n+3}{2}\,f(\eta) + \frac{n-1}{2}\,\eta\,f'(\eta)\right). \end{aligned}\right\} \qquad (7)$$

Equation (1) is identically satisfied on account of Eqs. (6) and (7), and Eqs. (2) to (5) are transformed to

$$f''' + \left(\frac{n+3}{2}\right)ff'' - n\,f'^2 - \left(M^* + \frac{1}{K^*}\right)f' = 0, \quad (8)$$

$$\left(1 + \frac{4}{3}R\right)\theta'' + Pr\left(\frac{n+3}{2}\right)f\,\theta' = 0, \qquad (9)$$

subject to the boundary conditions

$$\left.\begin{aligned} f(0) &= s^*,\ f'(0) = 1 + \mathcal{L}^* f''(0), \\ \theta(0) &= 1 + \delta^*\,\theta'(0), \\ f' &\to 0,\ \theta \to 0 \quad as\ \eta \to \infty. \end{aligned}\right\} \qquad (10)$$

Here $M^* = \sigma\,B_0^2 r^{1-n}/(\rho c)$ is the magnetic parameter; $K^* = k\,c\,r^{n-1}/(\nu\phi)$ is the permeability parameter; $R = 4\gamma^* T_\infty^3/(k_1 k^*)$ is the radiation parameter; $Pr = \mu c_p/k_1$ is the Prandtl number; $\mathcal{L}^* = l_1\sqrt{(c/\nu)}\,\sqrt{1/r^{1-n}}$ is the velocity slip parameter; $\delta^* = d_1\sqrt{c/\nu}\,\sqrt{1/r^{1-n}}$ is the thermal slip parameter, and $s^* = 2\,V_w r^{\frac{1-n}{2}}/((n+3)\sqrt{\nu c})$ is the mass transfer parameter, where $s^* > 0$ corresponds to suction and $s^* < 0$ corresponds to injection.

It should be noted that the occurrence of the radial co-ordinate (r) in the expressions of $M^*, K^*, \mathcal{L}^*$ and δ^* and the presence of radial co-ordinate (r) and stretching parameter (n) in s^* tend to break down the similarity solution. Concentrating on the expressions of $M^*, K^*, \mathcal{L}^*$, δ^* and s^*, two types of special terms P_{nr} and P'_{nr} (cf. Yazdi *et al.*, 2011) can be seen, where

$$P_{nr} = r^{1-n} \text{ and } P'_{nr} = \frac{4}{n+3}\sqrt{P_{nr}}.$$

Here, P_{nr} appears in $M^*, K^*, \mathcal{L}^*, \delta^*$ and P'_{nr} in s^*. These parameters oblige our Eqs. (8-10) to be solved locally. It is noted that P_{nr} and P'_{nr} are equal to 1 in the linear stretching sheet problem i.e. $n = 1$. Rewriting of the expressions of $M^*, K^*, \mathcal{L}^*, \delta^*$ and s^* based on the terms P_{nr} and P'_{nr} yields expressions of $M, K, \mathcal{L}, \delta$ and s independent from r and n as follows:

$$M^* = \frac{\sigma\,B_0^2}{\rho c}r^{1-n} = MP_{nr},\ K^* = \frac{k\,c}{\nu\phi}\left(\frac{1}{r^{1-n}}\right) = \frac{K}{\sqrt{P_{nr}}}, \mathcal{L}^* = l_1\sqrt{\left(\frac{c}{\nu}\right)}\sqrt{\frac{1}{r^{1-n}}} = \frac{\mathcal{L}}{\sqrt{P_{nr}}}, \delta^* = d_1\sqrt{\left(\frac{c}{\nu}\right)}\sqrt{\frac{1}{r^{1-n}}} = \frac{\delta}{\sqrt{P_{nr}}}$$

$$\text{and } s^* = -\frac{2\,V_w r^{\frac{1-n}{2}}}{(n+3)\sqrt{\nu c}} = s\sqrt{P'_{nr}},$$

where $M, K, \mathcal{L}, \delta$ and s are magnetic, permeability, velocity slip, thermal slip and mass transfer parameters based on P_{nr} and P'_{nr}, which are totally independent from r and n Consequently, there is an appropriate possibility by defining these parameters $M, K, \mathcal{L}, \delta$ and s keeping away from the difficulties of the dependency of M^*, K^*, $\mathcal{L}^*$, δ^* and s^* on r and n. Thus, the local similarity solution of the problem for the fixed values of the r-coordinate by varying n would be obtained properly for the various values of the involved parameters of the problem for momentum and energy Eqs. (8-10).

The physical quantities of our interest are the skin friction coefficient C_f and the local Nusselt number Nu defined as

$$\boldsymbol{C_f} = \frac{\boldsymbol{\tau_w}}{\boldsymbol{\rho U^2/2}},\ \boldsymbol{Nu} = \frac{\boldsymbol{r q_w}}{\boldsymbol{k_1(T_w - T_\infty)}}, \qquad (11)$$

where $\boldsymbol{\tau_w}$ and $\boldsymbol{q_w}$ are the wall shear stress and wall heat flux:

$$\boldsymbol{\tau_w} = \boldsymbol{\mu}\left(\frac{\partial u}{\partial z}\right)_{z=0}, \boldsymbol{q_w} = -\left(\boldsymbol{k_1} + \frac{16\gamma^* T_\infty^3}{3k^*}\right)\left(\frac{\partial T}{\partial z}\right)_{z=0}. \quad (12)$$

In terms of the dimensionless variables defined in Eqs. (6) and (7), these quantities become

$$\frac{\boldsymbol{Re^{\frac{1}{2}}C_f}}{\boldsymbol{2}} = \boldsymbol{f''(0)},\ \boldsymbol{Re^{-\frac{1}{2}}Nu} = -\left(\boldsymbol{1} + \frac{\boldsymbol{4}}{\boldsymbol{3}}\boldsymbol{R}\right)\boldsymbol{\theta'(0)}.$$

The Eqs. (8) and (9) are highly non-linear similarity boundary layer equations to be solved by DTM -Pade treatment in the present paper.

III. PRINCIPLES OF ANALYTICAL METHODS

A. The Differential Transform Method

An arbitrary function $\boldsymbol{u(x)}$ analytic in the domain $\boldsymbol{D}$, can be written in the Taylor series form about $\boldsymbol{x = x_0}$, as

$$\boldsymbol{u(x)} = \sum_{k=0}^{\infty} \frac{1}{k!}\left[\frac{d^k u(x)}{dx^k}\right]_{x=x_0} (\boldsymbol{x}-\boldsymbol{x_0})^{\boldsymbol{k}}, \boldsymbol{x} \in \boldsymbol{D} \quad (13)$$

The differential transform of $\boldsymbol{u(x)}$ is defined as

$$\boldsymbol{U(k)} = \frac{1}{k!}\left[\frac{d^k u(x)}{dx^k}\right]_{x=x_0}, \quad (14)$$

where $\boldsymbol{u(x)}$ is the original function and $U(k)$ is the transformed function.

The inverse differential transform is defined as

$$\boldsymbol{u(x)} = \sum_{k=0}^{\infty} \boldsymbol{U(k)}(\boldsymbol{x}-\boldsymbol{x_0})^{\boldsymbol{k}}. \quad (15)$$

In actual applications, the function $\boldsymbol{u(x)}$ is expressed by a finite series and hence Eq. (15) can be taken as follows:

$$\boldsymbol{u(x)} \approx \sum_{k=0}^{m} \boldsymbol{U(k)}(\boldsymbol{x}-\boldsymbol{x_0})^{\boldsymbol{k}},$$

where $\sum_{k=m+1}^{\infty} \boldsymbol{U(k)}(\boldsymbol{x}-\boldsymbol{x_0})^{\boldsymbol{k}}$ is negligibly small. Usually, the value of $\boldsymbol{m}$ is decided by the convergence of the series coefficient.

B. Pade Approximant

Let the power series $\sum_{i=0}^{\infty} a_i\, x^i$ represent the function $f(x)$ such that

$$f(x) = \sum_{i=0}^{\infty} a_i\, x^i. \quad (16)$$

The Pade approximant (cf. Baker, 1975; and Baker and Morris, 1996) is a rational function given by

$$[L/M] = \frac{P_L(x)}{Q_M(x)}, \quad (17)$$

where $P_L(x)$ is a polynomial of degree atmost L and $Q_M(x)$ is a polynomial of degree atmost M.

And we have

$$f(x) = a_0 + a_1x + a_2x^2 + a_3x^3 + \dots, \quad (18)$$

$$P_L(x) = p_0 + p_1x + p_2x^2 + \dots + p_Lx^L, \quad (19)$$

$$Q_M(x) = q_0 + q_1x + q_2x^2 + \dots + q_Mx^M. \quad (20)$$

Thus, there are $L+1$ numerator and $M+1$ denominator coefficients in Eq. (17). Since numerator and denominator of Eq. (17) can be multiplied by a constant in such a way that the Pade approximant $[L/M]$ is left unchanged, the normalization condition

$$Q_M(0) = 1, \quad (21)$$

is worth imposing in the analysis.

As a result, the number of independent numerator and independent denominator coefficients become $L+1$ and M, respectively, thereby making the total number of unknown coefficients equal to $L+M+1$. This number suggests that the Pade approximant $[L/M]$ normally ought to fit the power series given by relation (16) through the orders $1, x, x^2, x^3, \dots, x^{1+M}$.

Furthermore, the power series given by the relation (16) can be expressed formally as

$$\sum_{i=0}^{\infty} a_i\, x^i = \frac{p_0 + p_1x + p_2x^2 + \dots + p_Lx^L}{q_0 + q_1x + q_2x^2 + \dots + q_M\, x^M} + O(x^{L+M+1}). \quad (22)$$

By cross multiplying, we get that

$$(a_0 + a_1x + a_2x^2 + a_3x^3 + \dots)(q_0 + q_1 + q_2x^2 + \dots + q_Mx^M) = p_0 + p_1x + p_2x^2 + \dots + p_Lx^L + O(x^{L+M+1}) \quad (23)$$

Equating the coefficients of $1, x, x^2, x^3, \dots, x^L$ and the coefficients of $x^{L+1}, x^{L+2}, \dots, x^{L+M}$, we get the following sets of equations:

Table1. The operations for the one-dimensional differential transform method

Original function	Transformed function
$u(x) = u_1(x) \pm u_2(x)$	$U(k) = U_1(k) \pm U_2(k)$
$u(x) = \lambda\, u_1(x)$	$U(k) = \lambda U_1(k)$, λ is a constant
$u(x) = \frac{du_1(x)}{dx}$	$U(k) = (k+1)U_1(k+1)$
$u(x) = \frac{d^r u_1(x)}{dx^r}$	$U(k) = (k+1)(k+2)\cdots(k+r)U_1(k+r)$
$u(x) = u_1(x)u_2(x)$	$U(k) = \sum_{r=0}^{k} U_1(r)U_2(k-r)$
$u(x) = \frac{du_1(x)}{dx} \times \frac{du_2(x)}{dx}$	$U(k) = \sum_{r=0}^{k} (r+1)(k-r+1)\, U_1(r+1)U_2(k-r+1)$
$u(x) = u_1(x)\frac{du_2(x)}{dx}$	$U(k) = \sum_{r=0}^{k} (k-r+1)U_1(r)\, U_2(k-r+1)$
$u(x) = u_1(x)\frac{d^2u_2(x)}{dx^2}$	$U(k) = \sum_{r=0}^{k} (k-r+2)(k-r+1)\, U_1(r)U_2(k-r+2)$

$$\left.\begin{array}{c} a_0 = p_0, \\ a_1 + a_0\, q_1 = p_1, \\ a_2 + a_1\, q_1 + a_0\, q_2 = p_2, \\ \vdots \\ a_L + a_{L-1}q_1 + a_{L-2}\, q_2 + \dots + a_0q_L = p_L \end{array}\right\} \quad (24)$$

and

$$\left.\begin{array}{c} a_{L+1} + a_Lq_1 + \dots + a_{L-M+1}q_M = 0, \\ a_{L+2} + a_{L+1}q_1 + \dots + a_{L-M+2}q_M = 0, \\ \vdots \\ a_{L+M} + a_{L+M-1}q_1 + \dots + a_Lq_M = 0. \end{array}\right\} \quad (25)$$

If $n < 0$, we take $a_n = 0$ for consistency and $q_j = 0$ for $j > M$.

On solving the Eqs. (24) and (25) directly, we obtain

$$[L/M] = \frac{\begin{vmatrix} a_{L-M+1} & a_{L-M+2} & \cdots & a_{L+1} \\ \vdots & \vdots & \ddots & \vdots \\ a_L & a_{L+1} & \cdots & a_{L+M} \\ \sum_{j=M}^{L} a_{j-M}x^j & \sum_{j=M-1}^{L} a_{j-M}x^j & \cdots & \sum_{j=0}^{L} a_{j-M}x^j \end{vmatrix}}{\begin{vmatrix} a_{L-M+1} & a_{L-M+2} & \cdots & a_{L+1} \\ \vdots & \vdots & \ddots & \vdots \\ a_L & a_{L+1} & \cdots & a_{L+M} \\ x^M & x^{M-1} & \cdots & 1 \end{vmatrix}}$$

The Eqs. (24) and (25) are used to determine the Pade numerator and denominator of Eq. (22), and they are also called Pade equations. The symbol [L/M] is called Pade approximant and it has been constructed in Eq. (26).

IV. APPLICATION

Taking the one-dimensional differential transform of each term of Eqs. (8) and (9) with the help of Table 1, the following transforms are obtained:

$$\left.\begin{array}{c} f''' \rightarrow (k+1)(k+2)(k+3)F(k+3) \\ f' \rightarrow (k+1)F(k+1) \\ f'^2 \rightarrow \sum_{r=0}^{k}(r+1)(k-r+1)F(r+1)F(k-r+1) \\ f\,f'' \rightarrow \sum_{r=0}^{k}(r+1)(r+2)F(r+2)F(k-r) \\ \theta'' \rightarrow (k+1)(k+2)G(k+2) \\ f\,\theta' \rightarrow \sum_{r=0}^{k}(k-r+1)F(r)G(k-r+1) \end{array}\right\} \quad (27)$$

where $F(k)$ and $G(k)$ are transformed functions of $f(\eta)$ and $\theta(\eta)$, respectively, and are given by

$$f(\eta) \approx \sum_{k=0}^{m} F(k)\eta^k, \quad \theta(\eta) \approx \sum_{k=0}^{l} G(k)\eta^k \quad (28)$$

On substituting the Eqs. (27) into Eqs. (8) and (9), we obtain

$$F(k+3) = -\frac{1}{(k+1)(k+2)(k+3)} \times \quad (29)$$

$$\left\{\sum_{r=0}^{k}\begin{bmatrix} \left(\frac{n+3}{2}\right)(r+1)(r+2)F(r+2)F(k-r) \\ -\,n(r+1)(k-r+1)F(r+1)F(k-r+1)\end{bmatrix} - \left(M+\frac{1}{K}\right)(k+1)F(k+1)\right\}.$$

$$G(k+2) = -\frac{1}{\left(1+\frac{4}{3}R\right)(k+1)(k+2)} \times$$

$$\left\{Pr\left(\frac{n+3}{2}\right)\sum_{r=0}^{k}(k-r+1)F(r)G(k-r+1)\right\}. \quad (30)$$

We can now consider the boundary conditions in Eq. (10) as follows also:

$$f(0) = s, \quad f'(0) = 1 + \mathcal{L}f''(0), \quad f''(0) = 2\alpha_1,$$
$$\theta(0) = 1 + \delta\,\theta'(0), \quad \theta'(0) = \alpha_2,$$

so that the differential transforms of these boundary conditions are

$$\left.\begin{array}{c} F(0) = s,\ F(1) = 1 + 2\mathcal{L}\alpha_1,\ F(2) = \alpha_1, \\ G(0) = 1 + \delta\,\alpha_2, G(1) = \alpha_2. \end{array}\right\} \quad (31)$$

From the relations (29), (30) and boundary conditions (31), we recursively calculate all the $F(k)$'s and $G(k)$'s and then substituting all the $F(k)$'s and $G(k)$'s into Eqs. (28), we have the following series solutions for f and θ:

$$f(\eta) \approx s + (1 + 2\mathcal{L}\,\alpha_1)\eta + \alpha_1\eta^2 + \quad (32)$$
$$\frac{1}{6}\left[-(n+3)\,s\,\alpha_1 + \left(M + \frac{1}{K}\right)(1 + 2\mathcal{L}\,\alpha_1) + n(1 + 2\mathcal{L}\,\alpha_1)^2\right]\eta^3 + \cdots\cdots$$

$$\theta(\eta) \approx 1 + \alpha_2\delta + \alpha_2\,\eta - \frac{1}{4(3+4R)} \quad (33)$$
$$\left(3Pr\,s\,\alpha_2\,(n+3)\right)\eta^2 + \frac{1}{8(3+4R)^2}(\mathrm{Pr}\,\alpha_2(n+3)[6 - 3Pr\,s^2\,(n+3) + 12\mathcal{L}\,\alpha_1\,8\,R\,(1 + 2\mathcal{L}\alpha_1)])\eta^3 + \cdots$$

Though the series solutions (32) and (33) have sufficient accuracy, these series exhibit divergent behaviour around infinity. As a matter of this fact, it is not possible to find an analytical solution by DTM which satisfies the conditions at infinity. So, it becomes essential to combine the series solutions (32) and (33)obtained by DTM with the Pade approximant so as to provide an effective tool to handle the present boundary value problem on the infinite domain. We have, therefore, applied the Pade approximation to expressions (32) and (33) by way of taking the asymptotic boundary conditions $f' \rightarrow 0$ and $\theta \rightarrow 0$ as $\eta \rightarrow \infty$, to obtain α_1 and α_2 in the present analysis. Since the higher order approximation produces better accuracy and the diagonal approximants (cf. Rashidi, 2009) are the most accurate approximants, we have here constructed a [15/15] diagonal Pade approximant.

V. RESULTS AND DISCUSSION

The non-linear Eqs. (8) and (9) along with the boundary conditions (10) have been solved analytically by the DTM-Pade technique for different values of the governing parameters. To have a better insight into the physical nature of the problem, the effects of magnetic parameter (M), permeability parameter (K), stretching parameter (n), Prandtl number (Pr), suction/injection parameter (s), velocity slip parameter $(\mathcal{L})$, thermal slip parameter (δ) and radiation parameter (R) on the flow and temperature fields are presented graphically in Figs. 2-14.

In Table 2, we have validated our results of skin friction coefficient $(f''(0))$ and local Nusselt number $(-\theta'(0))$ for different values of n, M, K, s and Pr for $\mathcal{L} = \delta = R = 0$, by comparing them with the corresponding results of Khan e*t al.* (2015b) who solved the same problem by HAM in the absence of slip effects and radiation parameter. The results have been found in good agreement. Table 2 shows that $f''(0)$ decreases along with increasing values of n, M and s, while it increases with the increasing values of K. It further shows that with

Table 2. Comparison of the values of skin friction coefficient $f''(0)$ and local Nusselt number $(\theta'(0))$ by DTM-Pade[15/15] with Khan *et al.* (2015b) by HAM for $L = \delta = R = 0$

n	M	K	s	Pr	$f''(0)$ Present	$f''(0)$ Khan *et al.* (2015b)	$-\theta'(0)$ Present	$-\theta'(0)$ Khan *et al.* (2015b)
0.5					-2.42877	-2.48103	0.914135	0.95552
1.0	1.0	0.5	0.5	0.7	-2.5965	-2.65449	1.02945	1.06456
2.0					-2.90747	-2.98934	1.29011	1.27601
	0.0				-2.21258	-2.22272	0.984915	0.97777
0.5	0.5	0.5	0.5	0.7	-2.31686	-2.35608	0.950959	0.96601
	1.0				-2.42877	-2.48103	0.914135	0.95552
		0.25			-2.90038	-2.91999	0.905357	0.92239
0.5	1.0	0.5	0.5	0.7	-2.42877	-2.48103	0.914315	0.95552
		1.0			-2.21258	-2.22272	0.984915	0.97777
			0.5		-2.42877	-2.48103	0.914135	0.95552
0.5	1.0	0.5	0.0	0.7	-1.94565	-1.98299	0.41259	0.47138
			-0.5		-1.58965	-1.57760	0.069228	0.07525
				0.7	---	---	0.914135	0.95552
0.5	1.0	0.5	0.5	1.0	---	---	1.28825	1.31649
				1.2	---	---	1.55879	1.54791

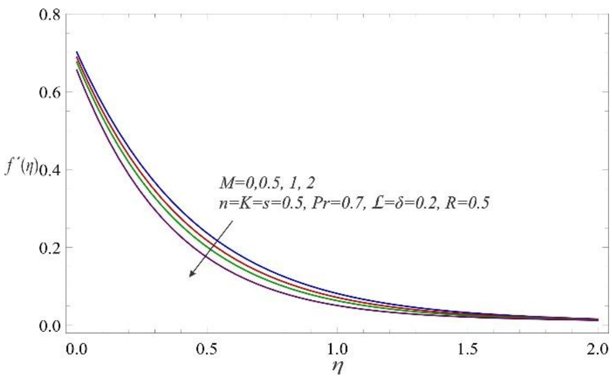

Figure 2: Effect of M on velocity distribution

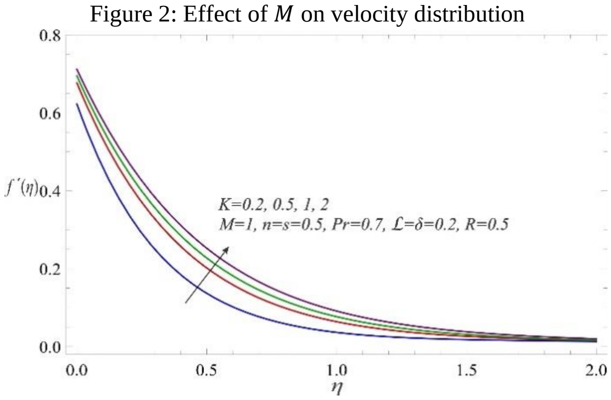

Figure 3: Effect of K on velocity distribution

an increase in $n,\ K,\ Pr$ and s, the local Nusselt number increases. But it decreases with an increase in M.

Figure 2 is drawn to see the effect of transverse magnetic field (M) on the velocity field ($f'(\eta)$) by keeping other parameters as fixed. It is seen from the figure that in case of suction, the momentum boundary layer thickness decreases with the increasing values of M. Thus, the flow rate decreases, thereby decreasing the velocity profiles. This happens due to the reason that the applied magnetic field to an electrically conducting fluid generates a drag like force called the Lorentz force, which has the ability to retard the velocity of the fluid in the boundary layer region.

Figure 3 elucidates that a rise in the value of permeability parameter (K) leads to a decrease of momentum boundary layer thickness. It can be observed from the expression of K that an increase in the value of K means an increase in the permeability of porous medium, hence, more space is available for the fluid to flow and thereby an increase in velocity is seen.

Figure 4 is plotted to see the effects of suction/injection parameter (s) on the velocity profile (($f'(\eta\ )$)). In case of suction ($s > 0$), the velocity distribution decreases with increasing values of s. But, in case of injection ($s < 0$), the velocity distribution increases with s. The stronger is the suction applied, the more is the fluid pushed towards the wall; thereby resulting into a decrease in the wall shear stress. This decrease in the wall shear stress causes a progressive thinning of the boundary layer. But, an opposite effect is observed in the flow field in case of injection.

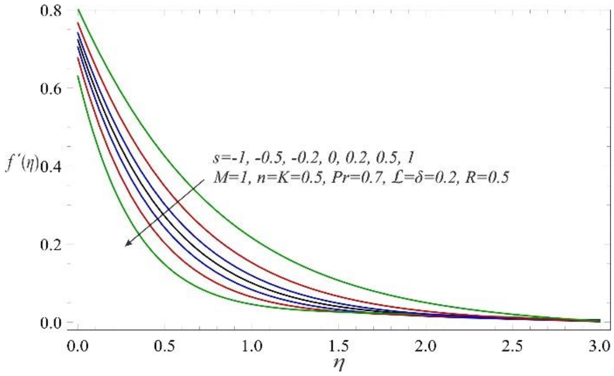

Figure 4: Effect of suction $s$on velocity distribution

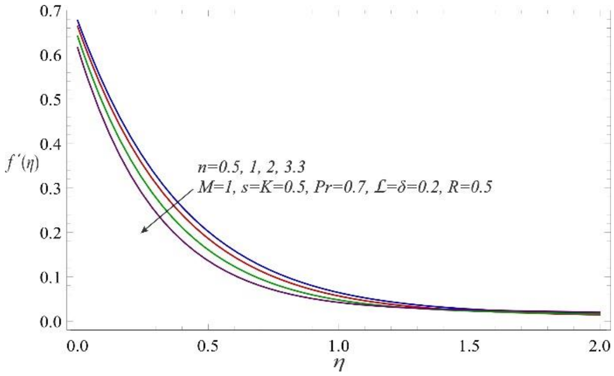

Figure 5 Effect of n on velocity distribution

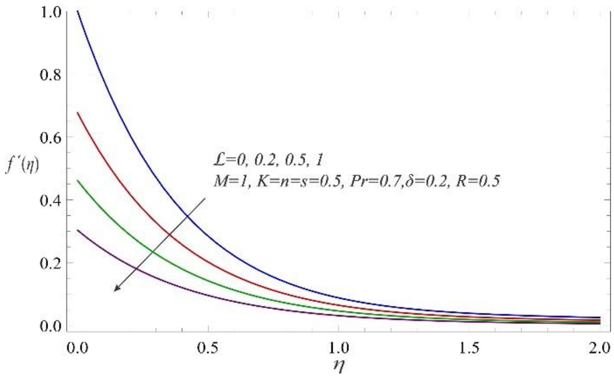

Figure 6: Effect of $\mathcal{L}$ on velocity distribution

The Fig. 5 shows the variation of velocity with stretching parameter (n). It is seen that the boundary layer thickness decreases with an increase in n due to the enhancement of momentum transfer.

The influence of slip parameter ($\mathcal{L}$) on the velocity profile ($f'(\eta)$) is shown in Fig. 6. It is seen that as the value of slip parameter increases, the boundary layer thickness decreases. As a result of this, the velocity profiles show a decreasing trend. This happens because the slip at the wall increases as the surface slip increases. As a consequence of this effect, only a very small amount of fluid is allowed to penetrate into the flow of the fluid over the surface of the stretching sheet. Thus, an enhancement in the value of slip parameter $\mathcal{L}$ means an enhancement of the slip between the surface of the sheet.

Figure 7 illustrates the effect of Prandtl number (Pr) on the temperature profile. From the figure, it is obvious that the thermal boundary layer thickness decreases along

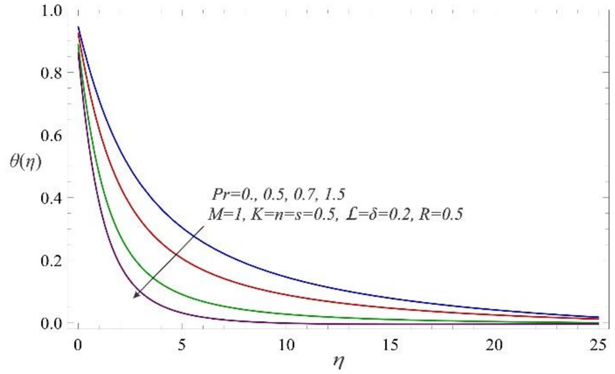

Figure 7: Effect of Pr on temperature distribution

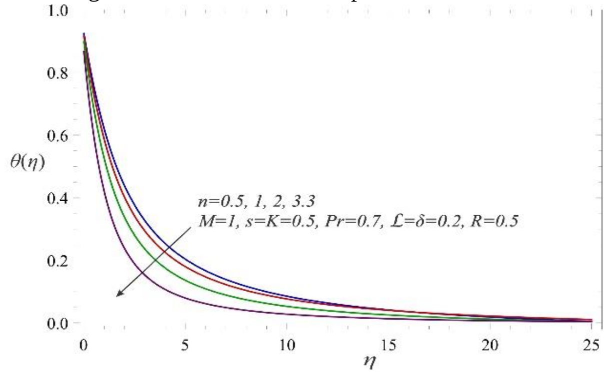

Figure 8: Effect of n on temperature distribution

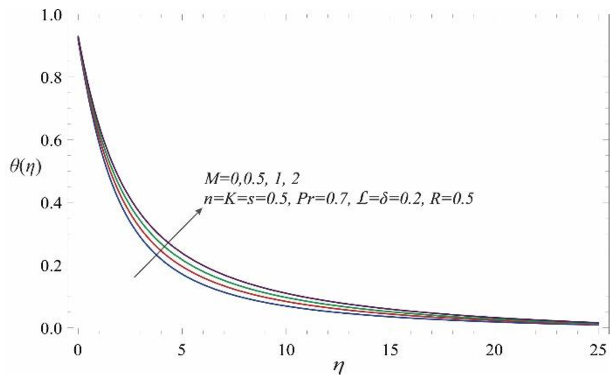

Figure 9: Effect of M on temperature distribution

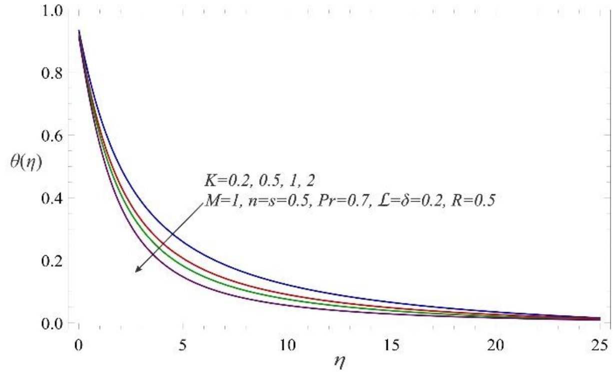

Figure 10: Effect of K on temperature distribution

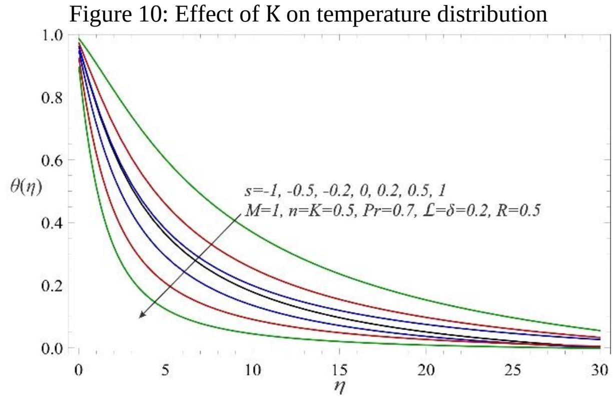

Figure 11: Effect of suction s on temperature distribution

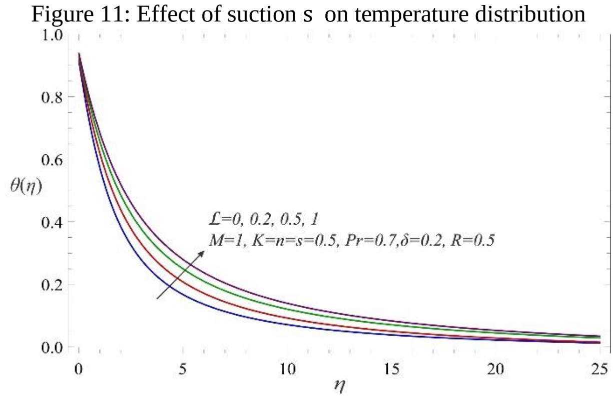

Figure 12 Effect of $\mathcal{L}$ on temperature distribution:

with the increasing values of Pr. As a result of this, the heat transfer at the wall also increases. This happens because the increasing values of Prandtl number cause an increase in the temperature gradient at the surface. This in turn results into an increase in the heat transfer rate at the surface. Thus, the higher values of Prandtl number show lower thermal diffusivity. This lower value of thermal diffusivity is responsible for a decay in the temperature profile.

Figure 8 illustrates the effects of stretching parameter (n) on the temperature field $(\theta(\eta))$. From the figure, it is found that the thermal boundary layer thickness decreases with an increase in n.

Figures 9-10 are sketched to see the effects of magnetic parameter (M) and permeability (K), respectively, on the temperature field. It is observed that as M increases, the thermal boundary layer thickness increases while it decreases with increasing K.

The effects of suction/injection parameter (s) on the temperature field are depicted in Fig. 11. It can be seen that the dimensionless temperature decreases as suction increases. But, a reverse trend is observed in case of injection. It is further observed that the effect of injection is more pronounced on the temperature field as compared to suction.

Figures 12 and 13 show the dimensionless temperature distribution for various values of velocity slip parameter $(\mathcal{L})$ and thermal slip parameter (δ), respectively. It is observed that with increasing values of $\mathcal{L}$, the fluid temperature increases. On the other hand, with an increase in the thermal slip parameter (δ), the fluid temperature decreases.

Figure 14 is plotted to see the effect of thermal radiation parameter (R) on the temperature distribution. From this figure, it is observed that the surface temperature $(\theta'(0))$ and the fluid temperature increase with an increase in thermal radiation. This is due to the fact that the

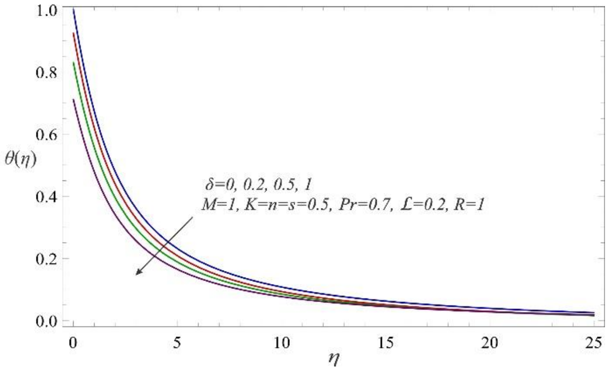

Figure 13: Effect of δ on temperature distribution

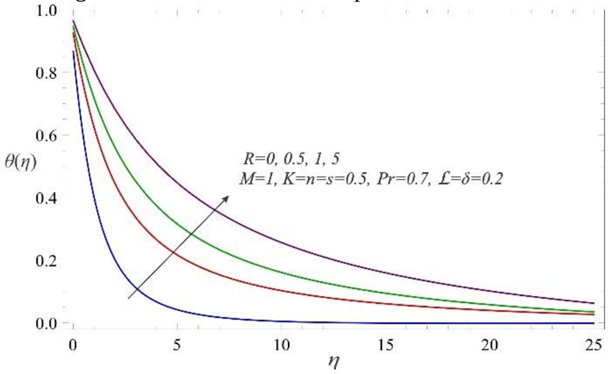

Figure 14: Effect of R on temperature distribution

divergence of the radiative heat flux (i.e. $\partial q_r/\partial r$) increases along with the decreasing values of the Rosseland radiative absorptivity (k_1). This, in turn, shows an increase in the rate of radiative heat transfer to the fluid. This causes the fluid temperature to increase. In view of this fact, the effect of radiation becomes more significant as $R \to \infty$, and the radiation effect is negligible as $R \to 0$.

VI. CONCLUSIONS

The MHD flow and heat transfer of an electrically conducting viscous fluid over a radially porous stretching power-law sheet in the presence of suction/injection parameter (s), thermal radiation (R), velocity slip $(\mathcal{L})$ and thermal slip (δ) effects are analyzed in the present study. The governing non-linear partial differential equations have been transformed to non-linear ODEs by using suitable similarity transformations, which are solved analytically by DTM-Pade method. To validate the accuracy of the numerical results obtained by the present method, a comparison has been made with the corresponding results of Khan *et al.* (2015b) (HAM). The results have been found in good agreement. The effects of various governing parameters on the flow and temperature fields have been studied graphically and the following conclusions are drawn from the analysis:

1. The boundary layer thickness and the flow velocity exhibit a decreasing trend with the increasing values of magnetic parameter (M), suction parameter (s), stretching parameter (n) and velocity slip parameter $(\mathcal{L})$.
2. The skin friction coefficient $(f''(0))$ shows an increasing trend with the increasing values of the magnetic parameter (M), suction/injection parameter (s) and the stretching parameter (n).
3. The velocity boundary layer thickness and flow velocity increase while the skin friction decreases with the increasing values of permeability parameter (K) and injection parameter (s).
4. The thermal boundary layer thickness and the fluid temperature decrease with an increase in Prandtl number (Pr), stretching parameter (n), permeability parameter (K), suction parameter (s) and thermal slip parameter (δ).
5. The local Nusselt number $(-\theta'(0))$ has an increasing effect with the increasing values of the parameters $Pr,\ n,\ K$ and s.
6. An increase in the magnetic number (M), injection parameter (s), velocity slip parameter $(\mathcal{L})$ and radiation parameter (R) results into an increases in the fluid temperature and thermal boundary layer thickness.
7. A decrease in the local Nusselt number is observed with an increase in the values of injection parameter (s) and magnetic parameter (M).
8. The numerical values obtained in the present analysis using DTM-Pade technique are in close agreement with the corresponding values obtained by a near-exact analytical technique called homotopy analysis method (HAM), thereby establishing the credibility, effectiveness and accuracy of DTM-Pade technique in solving the strongly nonlinear ordinary differential equations.

ACKNOWLEDGEMENT

The authors are highly obliged to Professor Ashok Kumar Singh; Ph.D. D.Sc., Head of the Department of Mathematics, Banaras Hindu University, Varanasi (India) for his painstaking guidance in the preparation of the manuscript of the present research paper.

REFERENCES

Abbas, Z., Wang Y., Hayat, T. and Oberlack, M. (2009). "Slip effects and heat transfer analysis in a viscous fluid over an oscillatory stretching surface," *International Journal for Numerical Methods in Fluids*, **59**, 443–458.

Ahmed, J., Mahmood, T., Iqbal, Z., Shahzad, A. and Ali, R. (2016). "Axisymmetric flow and heat transfer over an unsteady stretching sheet in power law fluid," *Journal of Molecular Liquids*, **221**,386–393.

Andersson, H. (1992). "MHD flow of a viscoelastic fluid past a stretching surface," *Acta Mechanica*, **95**, 227–230.

Andersson, H.I. (2002). "Slip flow past a stretching surface," *Acta Mechanica*, **158**, 121–125.

Ariel, P.D. (2001). "Axisymmetric flow of a second grade fluid past a stretching sheet," *International Journal of Engineering Science*, **39**, 529–553.

Ariel, P.D., Hayat, T. and Asghar, S. (2006). "The flow of an elastico-viscous fluid past a stretching sheet with partial slip," *Acta Mechanica*, **187**, 29–35.

Arikoglu, A. and Ozkol, I. (2006). "Solution of difference equations by using differential transform method," *Applied Mathematics and Computation*, **174**, 1216–1228.

Ayaz, F. (2004). "Solutions of the system of differential equations by differential transform method," *Applied Mathematics and Computation*, **147**, 547–567.

Baker, G.A. and Morris, G. (1996). *Encyclopedia of Mathematics and its Application*: *Parts I and II: Pad(́e) Approximants*, Addison-Wesley, New York.

Baker, G.A. (1975). *Essential of Padé Approximants*, Academic Press, New York.

Boyd, J.P. (1997). "Padé approximant algorithm for solving nonlinear ordinary differential equation boundary value problems on an unbounded domain," *Computers in Physics*, **11**, 299−303.

Brewster, M.Q. (1992). *Thermal Radiative transfer and properties*, John Wiley and Sons, New York.

Chen, C.K. and Char, M.I. (1988). "Heat transfer of a continuous, stretching surface with suction or blowing," *Journal of Mathematical Analysis and Applications*, **135**, 568–580.

Chen, C.K. and Huei, S.H. (1999). "Solving partial differential equations by two-dimensional differential transform method," *Applied Mathematics and Computation*, **106**, 171–179.

Cortell, R. (1994). "Similarity solutions for flow and heat transfer of a viscoelastic fluid over a stretching sheet," *International Journal of Non-Linear Mechanics*, **29**, 155–161.

Cortell, R. (2005). "Flow and heat transfer of a fluid through a porous medium over a stretching surface with internal heat generation/absorption and suction/blowing," *Fluid Dynamics Research*, **37**, 231–245.

Cortell, R. (2006). "Effects of viscous dissipation and work done by deformation on the MHD flow and heat transfer of a viscoelastic fluid over a stretching sheet," *Physics Letters A*, **357**, 298–305.

Crane, L.J. (1970). "Flow past a stretching plate," *Zeitschrift für angewandte Mathematik und Physik*, **21**, 645–647.

Darania, P. and Ebadian, A. (2007). "A method for the numerical solution of the integro-differential equations," *Applied Mathematics and Computation*, **188**, 657–668.

Das, S., Jana, R.N. and Makinde, O.D. (2017). "Slip flow and radiative heat transfer on a convectively heated vertical cylinder," *Journal of Engineering Physics and Thermophysics*, **90**, 568–574.

Gangadhar, K., Kumar, D.V., Ibrahim, S.M. and Makinde, O.D. (2018). "On spectral relaxation approach to radiating Powell-Eyring fluid flow over a stretching disk with Newtonian heating," *Defect and Diffusion Forum*, **387**, 461–473.

Gupta, P.S. and Gupta, A.S. (1977). "Heat and mass transfer on a stretching sheet with suction or blowing," *The Canadian Journal of Chemical Engineering*, **55**, 744–746.

Hayat, T., Waqas, M., Shehzad, S.A. and Alsaedi A. (2015). "MHD stagnation point flow of Jeffrey fluid by a radially stretching surface with viscous dissipation and Joule heating," *Journal of Hydrology and Hydromechanics*, **63**, 311–317.

Hayat, T., Abbas, Z. and Sajid, M. (2006). "Series solution for the upper-convected Maxwell fluid over a porous stretching plate," *Physics Letters A*, **358**, 396–403.

Hossain, M.A. and Takhar, H.S. (1996). "Radiation effect on mixed convection along a vertical plate with uniform surface temperature," *Heat and Mass Transfer*, **31**, 243–248.

Khan, M., Munir, A., Shahzad, A. and Shah, A. (2015a). "MHD flow and heat transfer of a viscous fluid over a radially stretching power-law sheet with suction/injection in a porous medium," *Journal of Applied Mechanics and Technical Physics*, **56**, 231–240.

Khan, M., Malik, R., Munir, A. and Shahzad, A. (2015b). "MHD flow and heat transfer of Sisko fluid over a radially stretching sheet with convective boundary conditions," *Journal of the Brazilian Society of Mechanical Sciences and Engineering*, **38**, 1279–1289.

Liao, S.J., (2003). "On the analytic solution of magnetohydrodynamic flows of non-Newtonian fluids over a stretching sheet," *Journal of Fluid Mechanics*, **488**, 189–212.

Magyari, E. and Keller, B. (1999). "Heat and mass transfer in the boundary layers on an exponentially stretching continuous surface," *Journal of Physics D: Applied Physics*, **32**, 577–585.

Makanda, G., Makinde, O.D. and Sibanda, P. (2013). "Natural Convection of Viscoelastic Fluid from a Cone Embedded in a Porous Medium with Viscous Dissipation," *Mathematical Problems in Engineering*, **2013**, 1–11.

Makinde, O.D. and Aziz, A. (2010). "MHD mixed convection from a vertical plate embedded in a porous medium with a convective boundary condition," *International Journal of Thermal Sciences*, **49**, 1813–1820.

Makinde, O.D. and Moitsheki, R.J. (2008). "On nonperturbative techniques for thermal radiation effect on natural convection past a vertical plate embedded in a saturated porous medium," *Mathematical Problems in Engineering*, **2008**, 1–11.

Makinde, O.D., Mabood, F., Khan, W. A. and Tshehla, M.S. (2016). "MHD flow of a variable viscosity nanofluid over a radially stretching convective surface with radiative heat," *Journal of Molecular Liquids*, **219**, 624–630.

Mukhopadhyay, S. and Gorla, R.S.R. (2012). "Effects of partial slip on boundary layer flow past a permeable exponential stretching sheet in presence of thermal radiation," *Heat and Mass Transfer*, **48**, 1773–1781.

Mukhopadhyay, S. (2009). "Effects of radiation and variable fluid viscosity on flow and heat transfer along a symmetric wedge," *Journal of Applied Fluid Mechanics*, **2**, 29-34.

Raptis, A. (1998). "Radiation and free convection flow through a porous medium," *International Communications in Heat and Mass Transfer*, **25**, 289–295.

Rashidi, M.M. (2009). "The modified differential transform method for solving MHD boundary-layer equations," *Computer Physics Communications*, **180**, 2210–2217.

Sahoo, B. (2010). "Effects of slip, viscous dissipation and Joule heating on the MHD flow and heat transfer of a second grade fluid past a radially stretching sheet," *Applied Mathematics and Mechanics*, **31**, 159–173.

Sajid, M., Ahmad, I., Hayat, T. and Ayub, M. (2008). "Series solution for unsteady axisymmetric flow and heat transfer over a radially stretching sheet," *Communications in Nonlinear Science and Numerical Simulation*, **13**, 2193–2202.

Sakiadis, B.C. (1961). "Boundary-layer behavior on continuous solid surfaces: II. The boundary layer on a continuous flat surface," *AIChE Journal*, **7**, 221–225.

Shahzad, A., Ali, R. and Khan, M. (2012). "On the Exact Solution for Axisymmetric Flow and Heat Transfer over a Nonlinear Radially Stretching Sheet," *Chinese Physics Letters*, **29**, p.084705.

Shateyi, S. and Makinde, O.D. (2013). "Hydromagnetic Stagnation-Point Flow towards a Radially Stretching Convectively Heated Disk," *Mathematical Problems in Engineering*, **2013**, 1–8.

Sibanda, P. and Makinde, O.D. (2010). "On steady MHD flow and heat transfer past a rotating disk in a porous medium with ohmic heating and viscous dissipation," *International Journal of Numerical Methods for Heat and Fluid Flow*, **20**, 269–285.

Sparrow, E.M. and Cess, R.D. (1970). *Radiation heat transfer*. Brooks Cole Publishing Company, Belmont, California.

Su, X.-H. and Zheng, L.-C. (2011). "Approximate solutions to MHD Falkner-Skan flow over permeable wall," *Applied Mathematics and Mechanics*, **32**, 401–408.

Turkyilmazoglu, M. (2015a). "Slip flow and heat transfer over a specific wedge: an exactly solvable Falkner–Skan equation," *Journal of Engineering Mathematics*, **92**, 73–81.

Turkyilmazoglu, M. (2015b). "Exact Multiple Solutions for the Slip Flow and Heat Transfer in a Converging Channel," *Journal of Heat Transfer*, **137,** 101301.

Turkyilmazoglu, M. (2019). "Latitudinally deforming rotating sphere," *Applied Mathematical Modelling*, **71**, 1-11.

Vafai, K., Hadim, H. and Howell, J.R. (2000). *Handbook of Porous Media,* Second Edition.

Vajravelu, K. and Cannon, J.R. (2006). "Fluid flow over a nonlinearly stretching sheet," *Applied Mathematics and Computation*, **181**, 609–618.

Yazdi, M.H., Abdullah, S., Hashim, I. and Sopian, K. (2011). "Slip MHD liquid flow and heat transfer over non-linear permeable stretching surface with chemical reaction," *International Journal of Heat and Mass Transfer*, **54**, 3214-3225.

Yoshimura, A. and Prud'homme, R.K. (1988). "Wall Slip Corrections for Couette and Parallel Disk Viscometers," *Journal of Rheology*, **32**, 53–67.

Zhou, J.K. (1986). *Differential transformation and its appliations for electric circuits*, Huazhong University Press, Wuhan, China.

Received: October 3, 2019
Sent to Subject Editor: October 10, 2019
Accepted: February 21, 2020
Recommended by Subject Editor: Gianfranco Caruso